SV40 Oncoproteins Enhance Asbestos-Induced DNA Double-Strand Breaks and Abrogate Senescence in Murine Mesothelial Cells

Jodie R. Pietruska and Agnes B. Kane

Brown University, Department of Pathology and Laboratory Medicine, Providence, Rhode Island

Abstract

SV40 virus has emerged as a potential cofactor with asbestos in the development of diffuse malignant mesothelioma, but its precise role in the pathogenesis of this tumor is unclear. SV40 large T antigen is known to inactivate cellular proteins involved in DNA damage and senescence, including p53 and pRb. We hypothesize that SV40 oncoproteins will sensitize mesothelial cells to DNA damage induced by asbestos or chemotherapeutic agents. SV40 oncoprotein expression in murine mesothelial cell lines enhanced spontaneous and asbestos-induced double-strand breaks, indicated by γ-H2AX foci, and potentiated micronucleus formation. Mesothelial cells exposed to asbestos or bleomycin for 96 h acquired senescent-like morphology and displayed elevated senescence-associated β-galactosidase activity, reduced bromodeoxyuridine (BrdUrd) incorporation, and reduced colony formation. SV40 oncoprotein expression abrogated the senescent phenotype, and transfected cell lines showed an increase in both BrdUrd incorporation and colony formation after prolonged DNA damage. Murine mesothelial cell lines lacking wild-type p53 due to a point mutation or gene rearrangement also failed to senesce in response to asbestos or chemotherapeutic agents. In addition, stress-induced senescence in human mesothelial cell lines was impaired by SV40 oncoprotein expression (MeT-5A), p53 small interfering RNA, or spontaneous p53 mutation (REN). These studies suggest that exposure to DNA-damaging agents can induce senescence in both murine and human mesothelioma cell lines and suggest a major, although not exclusive, role for p53 in this response. SV40 virus may contribute to mesothelioma progression by impairing stress-induced senescence, in part through p53 inactivation, thereby favoring survival and proliferation of mesothelial cells that have sustained DNA damage. [Cancer Res 2007;67(8):3637–45]

Introduction

Diffuse malignant mesothelioma arises from mesothelial cells lining the pleural, peritoneal, and pericardial cavities and is highly resistant to current therapies. No precursor lesion has been identified and mesotheliomas are rarely diagnosed until advanced stages; as a result, prognosis is poor and survival is limited to less than 1 year after diagnosis (1). Although studies have firmly established a link between mesothelioma and asbestos exposure (2), mesothelioma occurs in fewer than 10% of exposed individuals (3). Although the exact mechanism of mesothelioma pathogenesis is not fully understood, genotoxic effects of asbestos fibers are hypothesized to play a role (4). Exposure of mesothelial cells to biopersistent asbestos fibers can result in iron-catalyzed generation of free radicals during direct fiber-target cell interactions (reviewed in ref. 5). Alternatively, mesothelial cells may be damaged indirectly by reactive oxygen species released by chronic inflammatory cells (5). Although asbestos fibers have been shown to induce DNA breakage and chromosomal damage in human and rodent mesothelial cells *in vitro* (6, 7), recent work suggests that asbestos may also promote survival of damaged mesothelial cells via induction of tumor necrosis factor-α and nuclear factor-κB (NF-κB; ref. 8). SV40 virus has been proposed to act as a cofactor with asbestos in mesothelioma pathogenesis, potentially through inactivation of the p53 and pRb tumor suppressor gene products and up-regulation of signaling pathways associated with immortalization and survival (9, 10).

p53 and pRb play central roles in cellular responses to DNA damage, controlling pathways leading to cell cycle arrest, death by apoptosis, or senescence (11, 12). Unlike the majority of solid tumors, mesotheliomas rarely exhibit p53 mutations, and no pRb mutations have been described (13), although the presence of SV40 T antigen (Tag) in more than 50% of human mesotheliomas (14) is predicted to inactivate both p53 and pRb (15, 16). Additionally, several lines of evidence *in vitro* and *in vivo* suggest a role for p53 inactivation in mesothelioma pathogenesis. In human mesothelioma cell lines, inactivating point mutations of p53 are associated with loss of the G_1-S checkpoint following ionizing radiation (17), and a spontaneous p53 mutation in a murine mesothelial cell line resulted in increased micronucleus formation following exposure to crocidolite asbestos or ionizing radiation (18). p53 deficiency has been shown to increase the incidence and reduce the latency of asbestos-induced murine mesotheliomas (19), and Li-Fraumeni family members heterozygous for mutant p53 show a slightly increased risk of mesothelioma following asbestos exposure (20).

We hypothesize that inactivation of p53 and pRb by SV40 Tag would potentiate DNA damage induced by asbestos fibers or chemotherapeutic agents. Asbestos fibers have been shown to induce DNA damage, cell cycle arrest (8), DNA repair activity (21), and apoptosis (22) in mesothelial cells. Chemotherapeutic agents, such as bleomycin or camptothecin, are used to target rapidly dividing tumor cells, although inactivation of pathways governing DNA damage response or apoptosis may enhance resistance to chemotherapy (23, 24). Although chemotherapeutic agents have been shown to induce telomere-independent (stress-induced) senescence in human and rodent cells (25), little is known about the ability of asbestos fibers to induce this response in mesothelial cells. In this study, we sought to investigate the consequences of SV40 oncoprotein expression and p53 inactivation on the fate of mesothelial cells exposed to asbestos fibers or chemotherapeutic agents.

Requests for reprints: Agnes B. Kane, Department of Pathology and Laboratory Medicine, Brown University, Box G-E534, Providence, RI 02912. Phone: 401-863-1110; Fax: 401-863-9008; E-mail: Agnes_Kane@brown.edu.

doi:10.1158/0008-5472.CAN-05-3727

Materials and Methods

Cell culture and transfections. Murine mesothelial cell lines D9 and D7 and malignant mesothelioma cell lines (7, 40) were isolated as described previously (18, 26). SV40-transformed fibroblasts (SVT2), SV40-immortalized human mesothelial cells (MeT-5A), and a human mesothelioma cell line (H28) were obtained from the American Type Culture Collection (Manassas, VA). The REN human mesothelioma cell line was a generous gift of Dr. Steven Albelda (University of Pennsylvania, Philadelphia, PA). D9, 40, 7, 7T, and SVT2 cells were maintained in DMEM with 10% fetal bovine serum (FBS, Atlanta Biologicals, Lawrenceville, GA), 2 mmol/L L-glutamine, 1 mmol/L sodium pyruvate, 10 units/mL/10 μg/mL penicillin/streptomycin, and 10 μg/mL gentamicin. D7 and D7T cells were maintained in DMEM/F-12 supplemented as above, with 1.25% Medium 199, 2 ng/mL epidermal growth factor, and 0.04% insulin/transferrin/selenium (Sigma, St. Louis, MO). H28 and REN cells were maintained in RPMI 1640 with 10% FBS, 2 mmol/L L-glutamine, 1 mmol/L sodium pyruvate, and penicillin/streptomycin. MeT-5A was maintained in DMEM/F-12 with 10% FBS and penicillin/streptomycin. Cells were maintained in a humidified atmosphere at 37°C, 94% air/6% CO_2. D7 and 7 cells were cotransfected with pSP189, which encodes SV40 large and small Tags (generously provided by Dr. Anatoly Zhitkovich, Brown University, Providence, RI; ref. 27), and pTK-Hygro (Clontech, Palo Alto, CA) using SuperFect (Qiagen, Valencia, CA), and stable subclones were isolated following selection with 500 μg/mL hygromycin B (Sigma).

Growth characteristics and treatments of mesothelial cell lines. Cell counts were done in triplicate using phase-contrast microscopy to determine doubling time. Crocidolite asbestos fibers obtained from stocks originally prepared and characterized by the International Union Against Cancer were purchased from Duke Scientific (Palo Alto, CA). Fiber lengths ranged from 0.1 to >35 μm (28). Murine cells were exposed to asbestos or bleomycin sulfate (LKT Labs, St. Paul, MN) in serum-free phenol red–free RPMI 1640 supplemented as for normal growth medium; cells were exposed to topotecan (LKT Labs) in phenol red–free RPMI 1640/2% FBS. Human cells were exposed to chemotherapeutic agents in phenol red–free RPMI 1640/2% FBS, except for MeT-5A, which was treated in RPMI 1640/10% FBS.

Reverse transcription-PCR. Total RNA was isolated using Tri Reagent (Molecular Research Center, Inc., Cincinnati, OH), reprecipitated with 0.4 mol/L LiCl/50% isopropanol, washed in 80% ethanol, and resuspended in autoclaved 0.1% diethylpyrocarbonate-treated water. Total RNA was reverse transcribed using Moloney murine leukemia virus (Invitrogen, Carlsbad, CA) and 0.5 mmol/L deoxynucleotide triphosphate (Promega, Madison, WI) for 30 min at 42°C. PCR was done using 200 ng cDNA per 20 μL reaction containing 1.0 mmol/L $MgCl_2$ and 100 nmol/L each of forward and reverse primers. Reactions were heated to 95°C for 5 min, cycled at 95°C (30 s), 60°C (30 s), and 72°C (90 s) for 30 cycles, and incubated at 72°C for 10 min. PCR products were separated on 3% agarose gels and visualized by ethidium bromide staining.

Western blotting. Equal quantities of protein were electrophoresed in 2× Laemmli buffer, transferred to Immobilon-FL polyvinylidene difluoride membranes (Millipore, Billerica, MA), and blotted for SV40 oncoproteins (pAb 108; 1:100), p53 (FL-393; 1:1,000 or DO-1; 1:1,000; Santa Cruz Biotechnology, Santa Cruz, CA) γ-tubulin (GTU-88; 1:5,000; Sigma), or β-actin (AC-15; 1:1,000; Sigma). Visualization and densitometry were done using the LiCOR Odyssey Infrared Imaging System and software (LiCOR, Lincoln, NE).

Coimmunoprecipitation. After preclearing with mouse serum (Sigma) or rabbit serum (Vector Laboratories, Burlingame, CA) and 1:1 Protein A/G Agarose (Santa Cruz Biotechnology), protein extracts were incubated overnight with primary antibody (FL-393 or pAb 108) and 1:1 Protein A/G Agarose. After centrifugation and washes in radioimmunoprecipitation assay buffer and PBS, pellets were resuspended in 2× Laemmli buffer and resolved using SDS-PAGE.

Immunofluorescence. Cells were fixed in 2% paraformaldehyde, permeabilized in 1% Triton X-100, and blocked in 5% normal goat serum/0.1% BSA/0.1% Tween 20. After incubation in primary antibody (pAb 108 or Ab-4; 1:500; Calbiochem, San Diego, CA) and Alexa Fluor 488 goat anti-mouse IgG (1:1500; Invitrogen), coverslips were stained with 300 nmol/L 4′,6-diamidino-2-phenylindole (DAPI) and visualized using fluorescence microscopy. For γ-H2AX immunofluorescence, 0.5% Triton X-100 permeabilizations were included after the primary and secondary antibodies. Foci were counted in a minimum of 100 cells per coverslip using confocal microscopy and Renaissance 410 software (Microcosm, Inc. Columbia, MD).

Nuclear aberrations and cell viability. Cells were exposed to 10 $\mu g/cm^2$ asbestos or 1 μg/mL bleomycin sulfate for 24 to 96 h, centrifuged to pellet floating cells, and fixed in 2% paraformaldehyde. Cells were permeabilized and stained with DAPI before scoring for micronuclei and apoptotic nuclei. Cell viability was quantitated using 400 nmol/L calcein AM (Invitrogen) and a SpectraMax M2 fluorescence microtiter plate reader (Molecular Devices, Sunnyvale, CA), with excitation/emission at 485/525 nm.

Senescence-associated β-galactosidase activity. Senescence-associated β-galactosidase (SA β-gal) staining was done as described by Dimri et al. (29) and incubated for 6 h (MeT-5A) or 24 h at 37°C in the absence of CO_2. A minimum of 300 cells per coverslip was scored for senescent morphology and cytoplasmic blue staining using bright-field and phase-contrast microscopy.

Bromodeoxyuridine incorporation. Cells were treated as indicated and 10 μmol/L bromodeoxyuridine (BrdUrd; Sigma) was added 1 h (murine cell lines) or 3 h (human cell lines) before fixation in 2% paraformaldehyde. Cells were permeabilized, blocked in 2% FBS/PBS, and incubated at 37°C in anti-BrdUrd (3D4; 1:200; PharMingen, San Jose, CA)/3% BSA/1 mmol/L $MgCl_2$/125 units/mL Benzonase (Sigma). After incubation with Alexa Fluor 488 goat anti-mouse IgG (1:1,000), cells were stained with DAPI. A minimum of 300 cells per coverslip was scored using fluorescence microscopy. For longer labeling, BrdUrd (1 μg/mL) and uridine (1 mg/mL; Sigma) were added 48 h before fixation.

Colony formation assay. Cells were trypsinized and viability was determined using trypan blue exclusion. Five hundred viable cells were replated into 100-mm dishes. After 6 days, colonies were fixed in methanol, stained with Giemsa (Sigma), and scored (>30 cells per colony). Growth properties of surviving cells were examined 6 days after replating onto coverslips and assessing for viability, BrdUrd incorporation, SA β-gal activity, or Tag expression.

Small interfering RNA knockdown of p53. The pSUPER.retro.puro knockdown constructs, containing hairpin sequences complementary to green fluorescent protein (GFP) or human p53, and retroviral packaging plasmids pVSV-G and pHIT60 were generously provided by Dr. Anatoly Zhitkovich. The packaging plasmids and knockdown constructs were cotransfected into the 293T packaging cell line using LipofectAMINE Plus (Invitrogen). Retroviral supernatants were collected 24 and 48 h post-transfection and incubated with the H28 cell line in the presence of 8 μg/mL polybrene (Sigma). Cells expressing GFP small interfering RNA (siRNA) or p53 siRNA were obtained following selection with 2.0 μg/mL puromycin (Sigma).

Results

Expression of SV40 oncoproteins alters growth properties of murine mesothelial cells. To investigate the effects of SV40 oncoprotein expression in mesothelial cells, we expressed SV40 large (Tag) and small (tag) Tags in preneoplastic (D7) and neoplastic (7) murine mesothelial cells. Consistent with their mesothelial origin, all cell lines expressed *WT1* mRNA (Fig. 1*A*). We compared the expression profiles of cell cycle regulatory genes implicated in the pathogenesis of malignant mesothelioma in D7, D7T, 7, and 7T cells and D9, an immortalized, nontumorigenic mesothelial cell line (18). Only D9 cells expressed $p16^{INK4a}$ (Fig. 1*A*), a cell cycle regulatory gene whose expression is lost in 60% to 100% of human mesotheliomas, most often due to small homozygous deletions (30). D9, D7, and the transfected cell line D7T retained expression of $p15^{INK4b}$ and $p19^{ARF}$ (Fig. 1*A*), the murine homologue

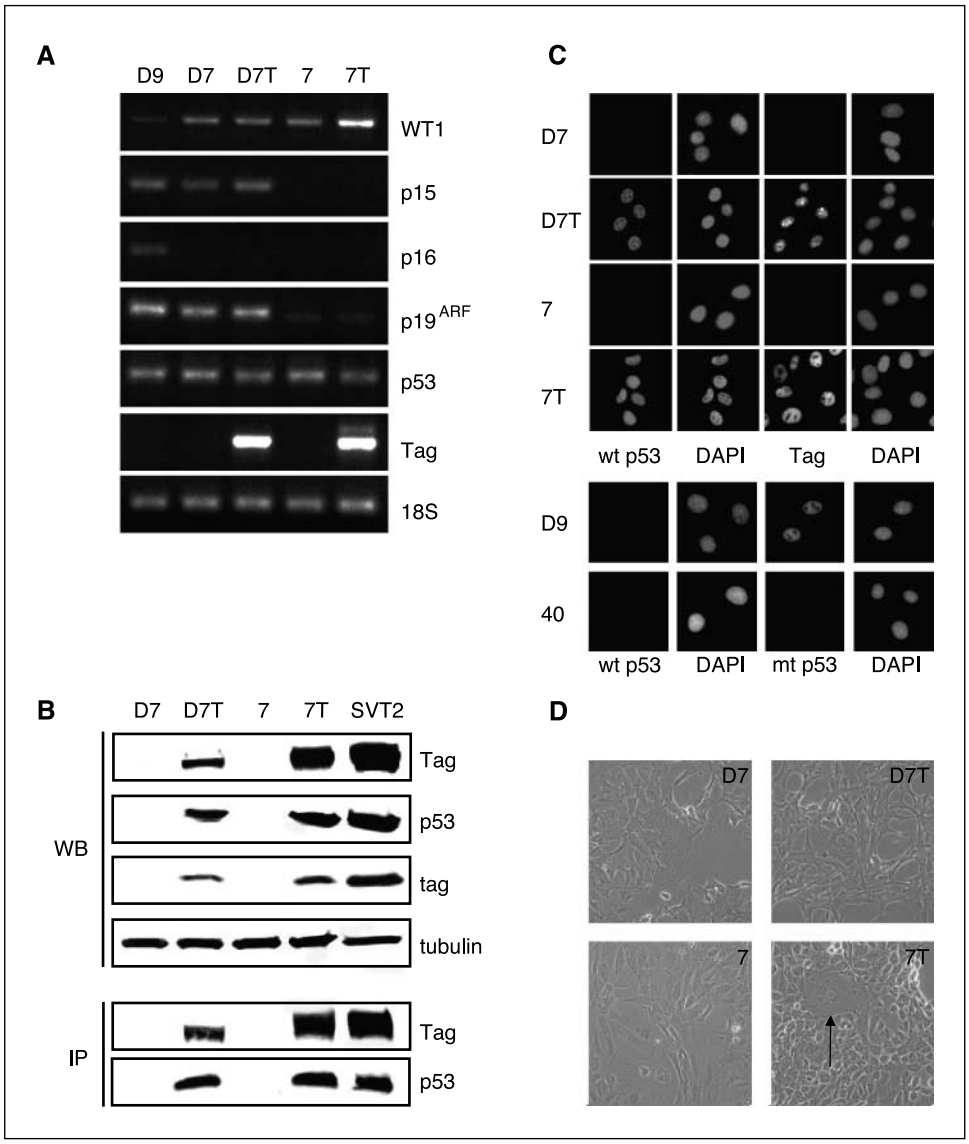

Figure 1. SV40 large Tag binds and stabilizes WT p53 in transfected mesothelial cells. *A,* reverse transcription-PCR analysis of tumor suppressor gene expression in immortalized mesothelial cells (*D9*), preneoplastic mesothelial cells (*D7*), mesothelioma cells (7), and transfected subclones of D7 and 7 (*D7T* and *7T*). Primers for 18S rRNA were included as an internal control. Reactions in which RNA or reverse transcriptase was omitted were included as negative controls (data not shown). *B,* Western blot showing expression of Tag and tag in transfected cells and SV40-transformed fibroblasts (*SVT2*). Blots were probed for γ-tubulin as a loading control. Coimmunoprecipitation/Western blot confirming interaction of Tag and p53. *C, top,* immunostaining showing nuclear localization of Tag and WT p53 in transfected cells; *bottom,* immunostaining of p53-deficient murine mesothelial cells. Experiments in which primary antibody was omitted were included as negative controls (data not shown). *D,* representative phase-contrast images of subconfluent cultured cells. Note the presence of large, multinucleated cells in 7T. Original magnification, ×200.

of human $p14^{ARF}$. In contrast, murine mesothelioma cell lines 7 and 7T did not express $p19^{ARF}$ (Fig. 1*A*), which is often codeleted with $p16^{INK4a}$ in human malignant mesotheliomas (31). All cell lines expressed *p53* (Fig. 1*A*), similar to the majority of human malignant mesotheliomas (13). As expected, D7T and 7T cells expressed *Tag* mRNA (Fig. 1*A*) and both large and small SV40 Tags (Fig. 1*B*). Large Tag localized to the nuclei of transfected cells (Fig. 1*C*), and its expression correlated with stabilization of wild-type (WT) p53 protein (Fig. 1*B* and *C*). Coimmunoprecipitation confirmed the interaction between Tag and WT p53 (Fig. 1*B*). An antibody specific for the mutant conformation of p53 was reactive only with D9 cells (Fig. 1*C*; ref. 18); the murine mesothelioma cell line, 40, did not express mutant or WT p53 (Fig. 1*C*).

Tag expression was also associated with morphologic alterations: D7T cells are smaller and more fibroblast-like than D7 cells (Fig. 1*D*), whereas 7T cells are smaller and more epithelial-like than 7 cells. Large, multinucleated cells were present in the 7T cell line under normal growth conditions (Fig. 1*D*). Consistent with the role of SV40 Tag in binding and inactivating cell cycle regulatory proteins to promote cell proliferation (32), SV40 oncoprotein expression was associated with reduced cell doubling time, from 17.5 to 14.0 h in preneoplastic mesothelial cells and from 17.1 to 8.9 h in mesothelioma cells. In addition, transfection of D7 cells with SV40 oncoproteins abrogated contact-inhibited cell growth, and both D7T and 7T cells grew to higher saturation densities than their respective parental cell lines (data not shown).

SV40 oncoproteins enhance asbestos and bleomycin-induced DNA damage. We predicted that inactivation of p53 by SV40 Tag would enhance DNA damage in mesothelial cells, as an inactivating p53 point mutation in a murine mesothelial cell line enhanced sensitivity to asbestos-induced micronuclei, as well as to ionizing radiation (18). Chinese hamster ovary cells deficient in double-strand break (DSB) repair show enhanced sensitivity to chrysotile asbestos, suggesting a role for DSB in asbestos-induced DNA damage (33). To examine the effect of SV40 oncoprotein expression on spontaneous and induced DSB, we compared phosphorylation of histone H2AX at COOH-terminal Ser^{139} in parental and transfected cell lines. Discrete foci containing phospho-H2AX (γ-H2AX) form rapidly after induction of DSB and are considered to be a sensitive and specific indicator of DSB (34).

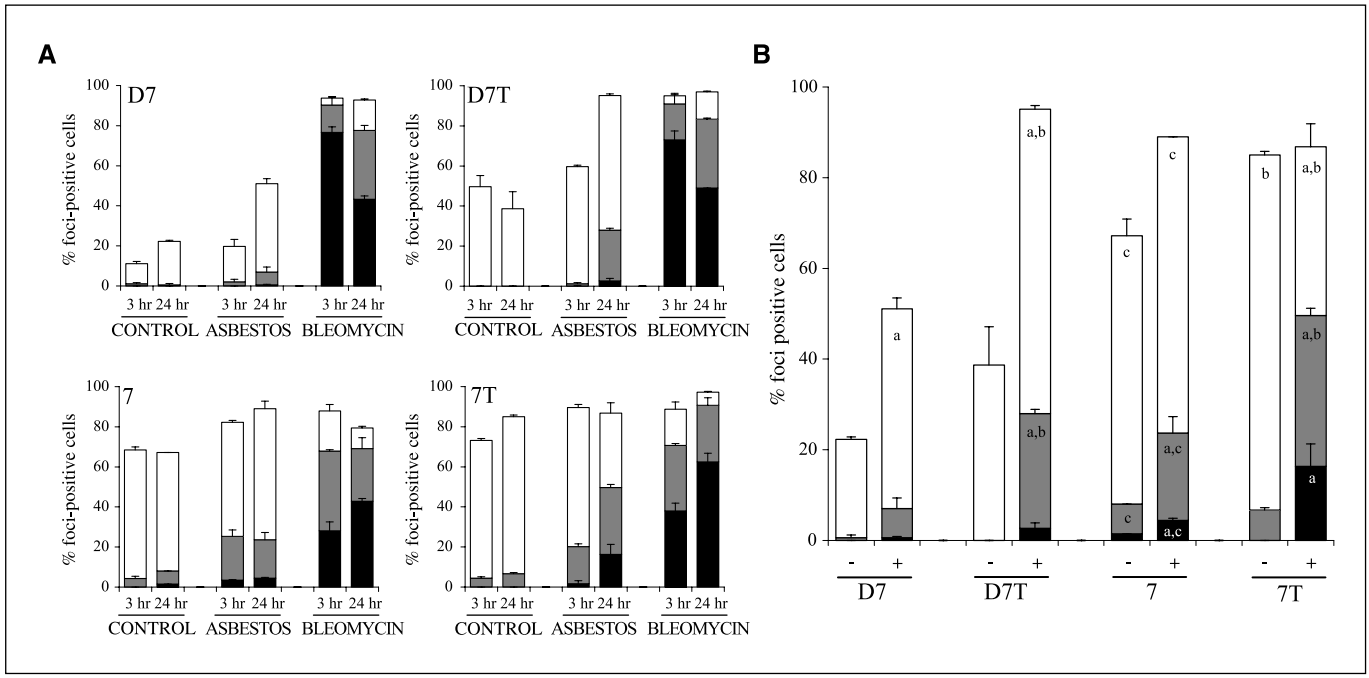

Figure 2. SV40 oncoproteins enhance spontaneous and asbestos-induced DNA DSBs. *A,* time course of γ-H2AX foci formation after asbestos or bleomycin exposure. Cells were exposed to 10 μg/cm^2 asbestos or 1 μg/mL bleomycin for 3 or 24 h. Cells were scored as having 1 to 10 (□), 11 to 20 (▩), or >20 (■) foci per cell. *Columns,* average percentage of cells in each category of three coverslips; *bars,* SE. *B,* statistical analysis of γ-H2AX foci formation after 24 h using Student's two-tailed *t* test ($P < 0.05$). *a,* difference between control (−) and asbestos (+) exposure is statistically significant; *b,* difference between transfected cell line and parental cell line is statistically significant; *c,* difference between neoplastic cell line and preneoplastic cell line is statistically significant.

We examined the consequences of SV40 oncoprotein expression on spontaneous DSB and on DSB induced by asbestos fibers or bleomycin, a radiomimetic chemotherapeutic agent that induces DSB via transition metal-dependent generation of free radicals (35). Relative to D7, increased spontaneous DSB were observed within 24 h in D7T as well as in both neoplastic cell lines (Fig. 2*A*). In both parental cell lines, asbestos fibers increased γ-H2AX foci within 24 h (Fig. 2*A* and *B*) and expression of SV40 oncoproteins increased sensitivity to asbestos-induced DSB in preneoplastic cells (Fig. 2*A* and *B*). Expression of SV40 oncoproteins in mesothelioma cells significantly increased the percentage of cells containing 11 to 20 foci and >20 foci (Fig. 2*B*). In contrast, although bleomycin produced DSB more rapidly and efficiently than asbestos, SV40 oncoproteins did not further increase bleomycin-induced DSB in either cell line (Fig. 2*A*). These results suggest that, in both preneoplastic and neoplastic mesothelial cell lines, SV40 oncoprotein expression potentiates asbestos-induced DSB. As persistent or unrepaired DSB could result in micronuclei and chromosomal aberrations, we examined formation of micronuclei in cell lines exposed to asbestos or bleomycin for 24, 60, or 96 h. SV40 oncoproteins enhanced asbestos-induced micronuclei in both preneoplastic and neoplastic cells and enhanced bleomycin-induced micronuclei only in preneoplastic cells (Fig. 3*A*).

SV40 oncoproteins alter toxicity in mesothelial cells exposed to asbestos or bleomycin. As DSB are considered to be the most lethal form of DNA damage, we compared cell viability during a 96-h exposure to asbestos fibers or bleomycin. D7 and 7 cells treated with asbestos or bleomycin showed a reduction in cell viability relative to untreated cells (Fig. 3*B*). SV40 oncoproteins protected from asbestos toxicity, particularly in preneoplastic mesothelial cells. In contrast, SV40 oncoprotein expression enhanced bleomycin toxicity in preneoplastic cells and only slightly decreased bleomycin toxicity in neoplastic cells. Consistent with a recent report showing increased resistance of human mesothelioma cells to asbestos-induced toxicity in the presence of Tag or SV40 (36), SV40 oncoprotein expression protected preneoplastic and, to a greater extent, neoplastic mesothelial cells from asbestos-induced apoptosis during a 96-h exposure. (Fig. 3*C*, compare *7* and *7T*). In contrast, transfected cell lines exhibited increased bleomycin-induced apoptosis compared with parental cell lines, especially at 60 and 96 h (Fig. 3*C*).

SV40 oncoproteins abrogate stress-induced mesothelial cell senescence. After prolonged exposure to asbestos or bleomycin, a subpopulation of parental cells displayed enlarged, flattened morphology characteristic of replicative or stress-induced senescence (37, 38) and elevated SA β-gal activity, which has been widely used as a marker of senescent cells in culture (29). After prolonged exposure to asbestos or bleomycin, both parental lines showed elevated SA β-gal activity relative to control cells (Fig. 4*B*), particularly in response to bleomycin. In contrast, transfected cell lines did not show senescent morphology or SA β-gal activity after asbestos or bleomycin treatment.

SA β-gal expression was accompanied by a decrease in BrdUrd incorporation in the parental cell lines (Fig. 4*B*), whereas the percentage of transfected cells undergoing DNA synthesis after a 96-h exposure to asbestos or bleomycin was significantly higher. We also assessed the colony-forming ability of surviving cells as an indicator of proliferative capacity after DNA damage. Preneoplastic and, to a lesser extent, neoplastic mesothelial cells showed a reduction in colony formation after treatment with asbestos or bleomycin (Fig. 4*C*). Consistent with the relative increase in BrdUrd incorporation in the presence of SV40 oncoproteins, transfected cell lines showed increased colony formation compared with parental lines, particularly in response to asbestos (Fig. 4*C*).

We observed two morphologically distinct populations of mesothelial cells that survived prolonged asbestos or bleomycin exposure. One population formed colonies with the morphology of growing, untreated cells (Fig. 4*D, right*), whereas a second population of enlarged, flattened cells failed to form colonies (Fig. 4*D, left*). This population was not observed in colony formation experiments using transfected cell lines, nor after replating untreated cells, indicating that failure to form colonies was not due to low plating density. Both populations were viable (Fig. 4*D*), and cells with senescent morphology expressed SA β-gal, whereas SA β-gal–positive cells were rarely observed in colonies of transfected cells and were most often large and multinucleated. As expected, cells growing in colonies incorporated BrdUrd (Fig. 4*D, right*), whereas isolated cells did not, even after a 48-h incubation (Fig. 4*D, left*), and all of the transfected cells growing in colonies retained Tag expression (Fig. 4*D, right*). In summary, prolonged DNA damage of murine mesothelial cells produces a subpopulation of isolated, enlarged cells that are viable but nonproliferating and senescent. In both preneoplastic and neoplastic cell lines, SV40 oncoprotein expression abrogated senescence induced in response to prolonged DNA damage.

Stress-induced senescence of human mesothelial cells is impaired by SV40 or p53 deficiency. To extend the relevance of our findings to human cell lines, we investigated stress-induced senescence in a SV40-negative human mesothelioma cell line (H28) and a SV40-immortalized human mesothelial cell line (MeT-5A). Following exposure to bleomycin or topotecan, a water-soluble camptothecin derivative, H28 showed similar dose-dependent increases in SA β-gal activity with concomitant decreases in BrdUrd incorporation (Fig. 5*A*). In contrast, SA β-gal activity in MeT-5A cells increased only

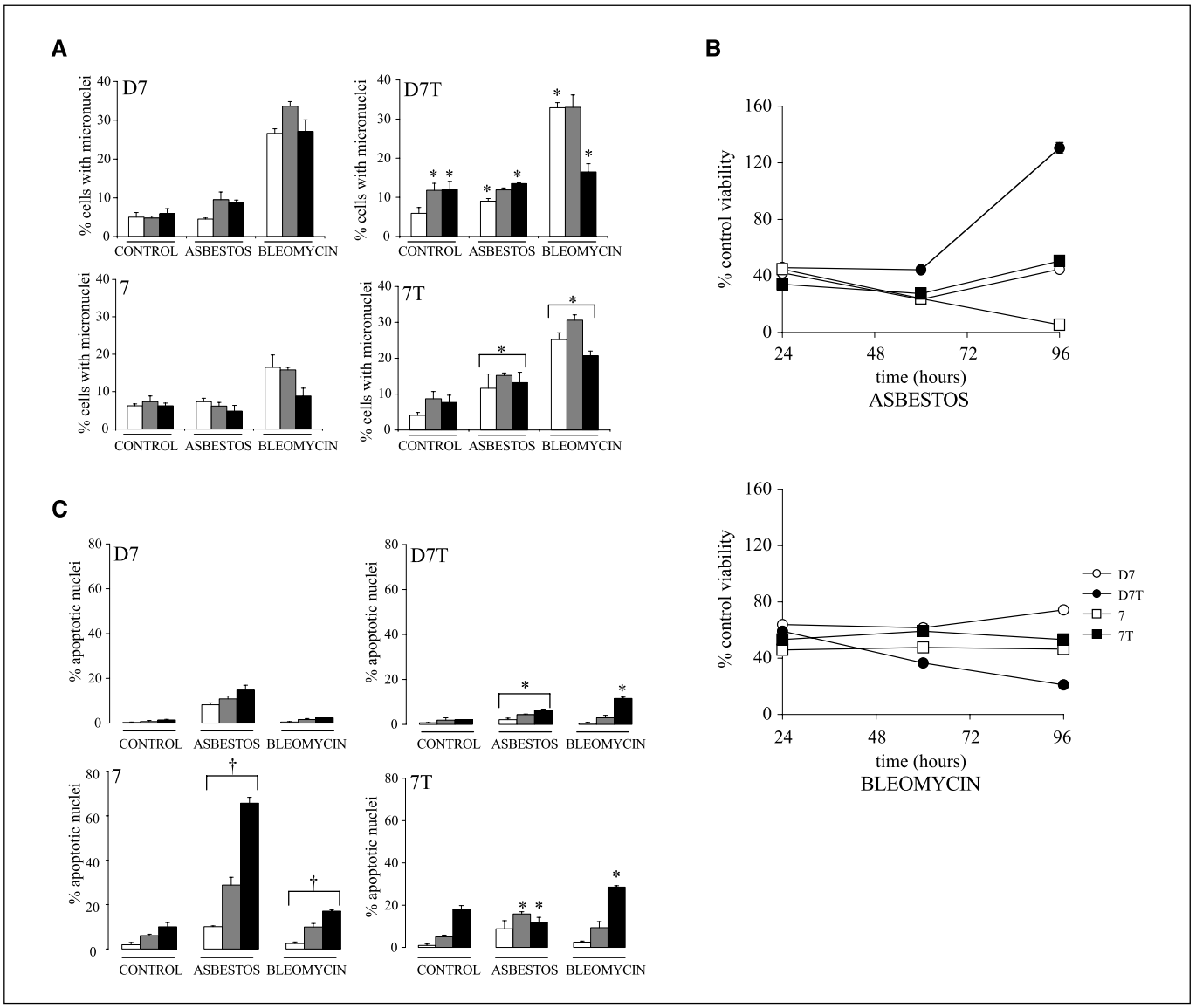

Figure 3. SV40 oncoproteins enhance spontaneous and induced micronuclei and protect mesothelial cells against asbestos-induced toxicity. *A,* formation of micronuclei during prolonged exposure to asbestos or bleomycin. Cells were exposed to 10 μg/cm^2 asbestos or 1 μg/mL bleomycin for 24 h (□), 60 h (▩), or 96 h (■). *Columns,* average of three coverslips; *bars,* SE. *, $P < 0.05$, significantly different from respective parental cell line, Student's two-tailed *t* test. *B,* calcein AM viability determination during asbestos (*top*) or bleomycin (*bottom*) exposure. *C,* prolonged DNA damage produces condensed, apoptotic nuclei during asbestos or bleomycin exposure. *Columns,* average of three coverslips; *bars,* SE. *, difference between transfected cell line and parental line is statistically significant; †, difference between preneoplastic cell line and neoplastic cell line is statistically significant.

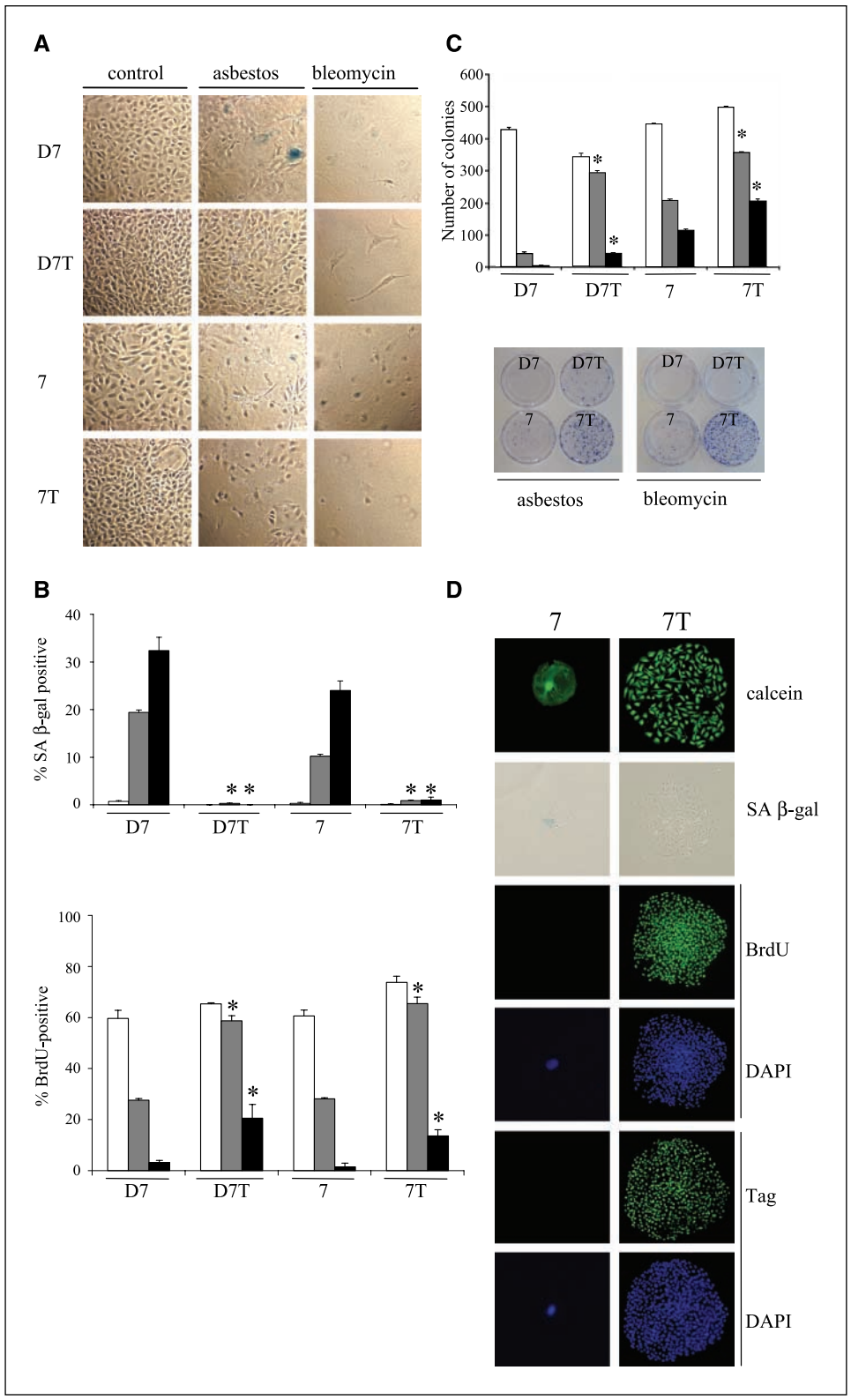

Figure 4. Persistent DNA damage induces a senescent phenotype in preneoplastic and neoplastic mesothelial cells that is abrogated by SV40 oncoprotein expression. *A,* representative images of morphology and SA β-gal activity in control cells or cells exposed to asbestos or bleomycin for 96 h. Original magnification of all images, ×200. *B* and *C,* untreated mesothelial cells (□) or mesothelial cells exposed to 10 μg/cm^2 asbestos (■) or 1 μg/mL bleomycin (■) for 96 h were assayed for SA β-gal activity (*B, top*), BrdUrd incorporation (*B, bottom*), or colony formation (*C*). *Columns,* average of three coverslips (*B*) or four replicate plates (*C*); *bars,* SE. *, $P < 0.05$, difference between transfected cell line and parental cell line is statistically significant, Student's two-tailed *t* test. *D,* phenotype of representative senescent (*7, left*) and proliferating cells (*7T, right*) surviving prolonged DNA damage. All images were obtained 6 d after plating for colony formation. Original magnification of all images, ×100.

slightly in response to either chemotherapeutic agent (Fig. 5*A*), and the percentage of treated MeT-5A cells undergoing DNA synthesis after 4 days remained similar to control. These results suggest that chemotherapeutic agents can also activate a senescence program in human mesothelial cells that is impaired by SV40 oncoproteins.

Both the p53 and pRb pathways have been implicated in stress-induced senescence, although DNA damage may preferentially engage the p53 pathway (39). We chose to address the role of p53 in mesothelial cell senescence based on the documented role of p53 in response to DNA damage, as well as on previous work suggesting a

role for p53 inactivation in asbestos-induced murine mesothelioma (19). Because Tag simultaneously inactivates both p53 and pRb, it was not possible to determine the relative contribution of each pathway to mesothelial cell senescence in SV40-positive cell lines. Consequently, we evaluated stress-induced senescence in two p53-deficient murine mesothelial cell lines: D9, which contains an inactivating p53 point mutation and expresses mutant p53 (Fig. 1*C*; ref. 18), and 40, a mesothelioma cell line that contains a *p53* gene rearrangement and lacks p53 expression entirely (Fig. 1*C*; ref. 26). Compared with D7, which expresses WT p53, D9 and 40 showed a drastic reduction in SA β-gal activity after exposure to agents capable of inducing DSB, including asbestos, bleomycin, and topotecan. (Fig. 5*B*). These results suggest a major, although not necessarily exclusive, role for p53 in stress-induced senescence in murine mesothelial cells.

The H28 mesothelioma cell line lacks expression of $p16^{INK4a}$ and $p14^{ARF}$ due to homozygous deletions in exons 1α and 1β of the INK4a/ARF locus but retains expression of WT p53 (40). The REN mesothelioma cell line, similar to the murine mesothelioma cell line 40, contains a rearranged *p53* gene and lacks expression of p53 protein (Fig. 5*C*; ref. 41) but retains an intact INK4a/ARF locus (41). Neither REN nor H28 cells expressed SV40 Tag mRNA or protein (data not shown). Topotecan induced p53 stabilization in H28 and produced a population of cells with senescent morphology and elevated SA β-gal activity within 4 to 6 days (Fig. 5*A* and *C*). In contrast, REN cells showed no elevation in p53 protein (Fig. 5*C*) or SA β-gal activity after a 4- to 6-day exposure to topotecan (Fig. 5*D*; data not shown).

To confirm a role for p53 in human mesothelioma cell senescence using isogenic cell lines, we stably expressed an siRNA construct targeting p53 in the H28 cell line. Compared with uninfected H28 cells or H28 cells expressing a construct targeting GFP, expression of a p53 siRNA construct resulted in decreased p53 mRNA levels (data not shown) and a >80% decrease in p53 protein levels on exposure to topotecan (Fig. 5*B*). To determine whether p53 expression was required for stress-induced senescence in H28 cells, populations of H28 cells expressing GFP siRNA or p53 siRNA were treated with 1.0 μmol/L topotecan for 6 days. The topotecan-induced increase in SA β-gal activity was comparable in uninfected H28 cells and in H28 cells expressing GFP siRNA, whereas expression of p53 siRNA was associated with decreased SA β-gal activity (Fig. 5*C*). Exposure to bleomycin also induced a senescent phenotype in H28 that was impaired in REN cells and after p53 knockdown (data not shown). These results suggest a major role for p53 in stress-induced senescence of human mesothelioma cells exposed to chemotherapeutic agents.

Discussion

In this study, we show that SV40 oncoprotein expression in preneoplastic and neoplastic murine mesothelial cells enhances both spontaneous and asbestos-induced DSB within 24 h, as well as micronuclei induced by exposure to asbestos or bleomycin. SV40 oncoprotein expression enhanced asbestos-induced micronuclei in both cell lines and increased bleomycin-induced micronuclei in the neoplastic mesothelial cell line after a 96-h exposure. SV40 Tag may potentiate DNA damage and genetic instability by inhibiting DNA repair directly through disruption of DNA repair foci (42) or indirectly by preventing p53-mediated cell cycle arrest and transcriptional activation of *p53* target genes involved in DNA repair (33). Alternatively, Tag has been shown to disrupt mitotic checkpoints necessary for maintenance of genomic stability (43). Although the oncogenic effects of SV40 have been mostly attributed to large Tag, several lines of evidence suggest a role for small tag in mesothelioma pathogenesis. Small tag is required for transformation of human mesothelial cells by SV40 (44) and for induction of mesotheliomas by SV40 virus in hamsters (45). Asbestos and tag have been shown to independently up-regulate activator protein-1 and NF-κB transcription factors (reviewed in ref. 46), which are associated with cell proliferation and cell survival, respectively. Therefore, it is possible that tag could further enhance proliferation and survival of mesothelial cells exposed to asbestos fibers. Recent reports have shown increased activity of the prosurvival Akt pathway in human and murine mesotheliomas (47), as well as higher Akt activity in SV40-positive human mesothelioma cell lines, leading the authors to suggest a correlation between SV40 virus and cell survival in asbestos-induced mesotheliomas (48). Although our studies did not specifically address the involvement of these or other prosurvival signaling pathways, SV40 oncoprotein expression was associated with enhanced long-term survival of preneoplastic and neoplastic mesothelial cells after exposure to asbestos fibers or to a chemotherapeutic agent.

DNA damage–induced senescence has been described both in normal human fibroblasts (49) and in cell lines derived from multiple human tumor types (39, 49). Little is known about stress-induced senescence in malignant mesothelioma, although SV40 infection of human mesothelial cells has been shown to bypass replicative senescence through a Tag-dependent up-regulation of telomerase (50). Both replicative (telomere-dependent) and stress-induced (telomere-independent) senescence are believed to involve the p16/pRb and ARF/p53 pathways, although few studies have addressed stress-induced senescence in either preneoplastic or neoplastic mesothelial cells. In this *in vitro* model of murine mesothelioma, we observed a senescent phenotype in both preneoplastic and neoplastic mesothelial cells that shares several characteristics with DNA damage–induced senescence: enlargement and flattening of cells, expression of SA β-gal, and reduced cell proliferation as assessed by BrdUrd incorporation and colony formation. This phenotype persisted after reculturing surviving cells under normal growth conditions, suggesting that this growth arrest may be permanent. Although these murine preneoplastic and neoplastic mesothelial cell lines lack p16 and $p16/p19^{ARF}$ expression, respectively, both cell lines undergo senescence in response to asbestos and, to a greater extent, bleomycin and topotecan. These findings do not exclude a role for the *INK4a/ARF* locus or pRb in mesothelial cell senescence but suggest that inactivation of p16 alone or p16 and $p19^{ARF}$ is insufficient to abrogate the stress-induced senescence response. On expression of SV40 oncoproteins, which would be expected to disrupt p53 and pRb directly, transfected mesothelial cells failed to senesce in response to asbestos fibers or bleomycin and continued to incorporate BrdUrd and proliferate.

The inverse correlation between stress-induced senescence and SV40 status was also observed in human cell lines exposed to chemotherapeutic agents. Compared with H28, which exhibited senescent morphology, elevated SA β-gal, and decreased DNA synthesis after exposure to topotecan or bleomycin, an SV40-immortalized human cell line (MeT-5A) exhibited only slight alterations in SA β-gal and BrdUrd incorporation. The selected dose ranges were sufficient to induce up to a 3-fold increase in micronuclei in MeT-5A (data not shown), indicating that the failure to senesce was not due to subgenotoxic doses of these chemotherapeutic agents. Although we observed an apparent higher background of SA β-gal activity in MeT-5A than other

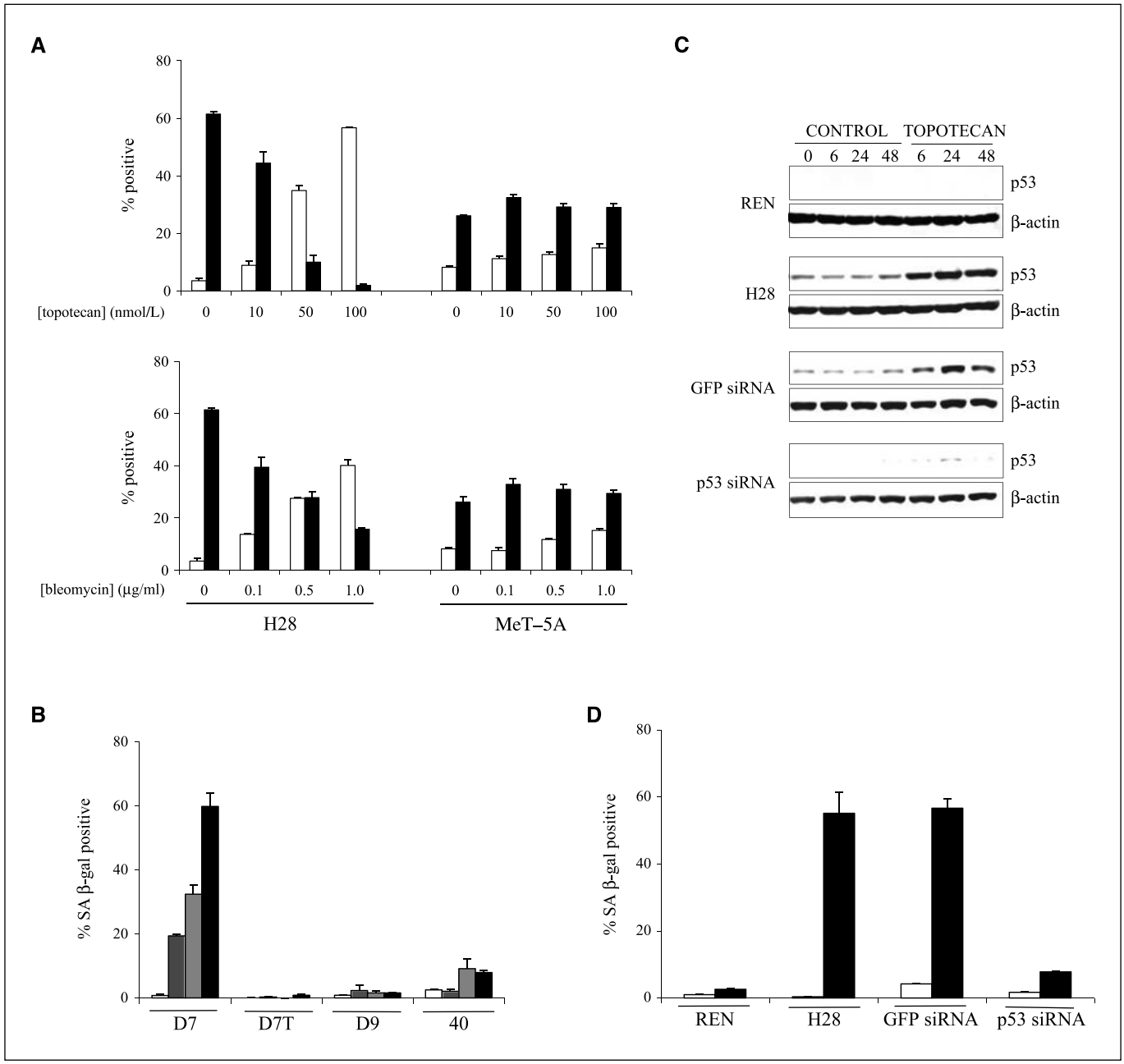

Figure 5. SV40 or p53 deficiency impairs stress-induced senescence in murine and human mesothelial cells. *A,* SV40-immortalized human mesothelial cells (MeT-5A) are impaired in stress-induced senescence. An SV40-negative human mesothelioma cell line (H28) and MeT-5A were evaluated for SA β-gal activity (□) and BrdUrd incorporation (■) following a 4-d exposure to the indicated doses of topotecan or bleomycin. *B,* inactivation of p53 in murine mesothelial cell lines is associated with decreased SA β-gal activity relative to control (□) after a 4-d exposure to asbestos (▨), bleomycin (▣), or topotecan (■). SA β-gal activity in D7 and D7T as shown in Fig. 4*B* is presented here for comparison. *C,* siRNA-mediated p53 knockdown in a WT p53 human mesothelioma cell line. Human mesothelioma cell lines with WT (H28) or mutated (REN) p53 and derivatives of H28 stably expressing GFP or p53 siRNA constructs were exposed to 1.0 μmol/L topotecan for the indicated times (h) and processed for Western blot analysis. *D,* p53 knockdown impairs stress-induced senescence in human mesothelioma cells. Following a 6-d exposure to control medium (□) or 1.0 μmol/L topotecan (■), cell lines and knockdown populations were assayed for SA β-gal activity. For all experiments, a minimum of 300 cells per coverslip was scored. *Columns,* average of three coverslips; *bars,* SE.

murine or human cell lines, we speculate that this is due to increased lysosomal mass in a subpopulation of large, multinucleated cells, as these cells express SV40 Tag and incorporate BrdUrd before and after exposure to chemotherapeutic agents (data not shown).

Cell lines with defined alterations in p53 were used to assess the contribution of p53 to stress-induced mesothelial cell senescence. Inactivation of p53 due to a point mutation (D9), gene rearrangement (40 and REN), or p53 siRNA (H28) compromised the senescence response, as evaluated by morphologic changes and SA β-gal activity. These results do not exclude a role for additional pathways that are targeted by SV40 Tag, such as pRb, which has been shown to play a direct role in DNA damage–induced senescence of human fibroblasts (51). Recent studies have provided convincing evidence for senescence *in vivo* and its role as a tumor suppression mechanism (52). These studies suggest that murine and human mesothelioma cells with WT p53 can undergo growth

arrest closely resembling senescence in response to chemotherapeutic agents. Although many chemotherapeutic agents induce apoptosis of tumor cells, the ability to undergo senescence is also an important determinant of treatment outcome (23, 51). Induction of senescence in mesothelioma cells expressing WT p53 may represent an alternative goal of chemotherapy, using doses that do not induce systemic toxicity. Although the majority of human mesotheliomas express WT p53, mesothelioma cells expressing mutant p53 or SV40 oncoproteins may be able to circumvent senescence induced by asbestos fibers or chemotherapeutic agents. Therefore, SV40 virus may enhance survival and proliferation of mesothelioma cells that would otherwise undergo senescence, which may have implications for treatment of mesotheliomas containing SV40, even if SV40 viral sequences are present in a subset of tumor cells. The ability of SV40 oncoproteins to bypass stress-induced senescence while promoting cell survival and growth after DNA damage suggests a novel mechanism by which SV40 virus could act as a cofactor with asbestos fibers in the development and progression of malignant mesothelioma.

Acknowledgments

Received 10/14/2005; revised 12/11/2006; accepted 2/8/2007.

Grant support: National Institute of Environmental Health Sciences grants RO1 ES03721 and T32 ES07272, National Cancer Center predoctoral fellowship (J.R. Pietruska), and Superfund Basic Research Program grant P42 ES013660.

The costs of publication of this article were defrayed in part by the payment of page charges. This article must therefore be hereby marked *advertisement* in accordance with 18 U.S.C. Section 1734 solely to indicate this fact.

References

1. Robinson BWS, Musk AW, Lake RA. Malignant mesothelioma. Lancet 2005;366:397 –408.
2. Craighead JE, Mossman BT. The pathogenesis of asbestos-associated diseases. N Engl J Med 1982;306: 1446–55.
3. Mossman B, Bignon J, Corn M, Seaton A, Gee J. Asbestos: scientific developments and implications for public policy Science 1990;247:294–301.
4. Kane A. Mechanisms of mineral fibre carcinogenesis. In: Kane AB, Boffetta P, Saracci R, Wilbourn J, editors. Mechanisms of fibre carcinogenesis. Vol. 140. Lyon: IARC Scientific Publications; 1996. p. 11–34.
5. Shukla A, Gulumian M, Hei TK, Kamp DW, Rahman Q, Mossman BT. Multiple roles of oxidants in the pathogenesis of asbestos-induced diseases. Free Radic Biol Med 2003;34:1117–29.
6. Pelin K, Husgafvel-Pursianinen K, Vallas M, Vanhala E, Linnainmaa K. Cytotoxicity and anaphase aberrations induced by mineral fibres in cultured human mesothelial cells. Toxicol In Vitro 1992;6:445–50.
7. Levresse V, Renier A, Levy F, Broaddus VC, Jaurand MC. DNA breakage in asbestos-treated normal and transformed (TSV40) rat pleural mesothelial cells. Mutagenesis 2000;15:239–44.
8. Yang H, Bocchetta M, Kroczynska B, et al. TNF-α inhibits asbestos-induced cytotoxicity via a NF-κB dependent pathway, a possible mechanism for asbestos-induced oncogenesis. Proc Natl Acad Sci U S A 2006;103:10397–402.
9. Rizzo P, Bocchetta M, Powers A, et al. SV40 and the pathogenesis of mesothelioma. Semin Cancer Biol 2001; 11:63–71.
10. Carbone MC, Kratzke RA, Testa JR. The pathogenesis of mesothelioma. Semin Oncol 2002;29:2–17.
11. Harris SL, Levine AJ. The p53 pathway: positive and negative feedback loops. Oncogene 2005;24:2899–908.
12. Campisi J. Cellular senescence as a tumor suppressor mechanism. Trends Cell Biol 2001;11:S27–31.
13. Metcalf RA, Welsh JA, Bennett WP, et al. *p53* and Kirsten-*ras* mutations in human mesothelioma cell lines. Cancer Res 1992;52:2610–5.
14. Testa JR, Carbone MC, Hirvonen A, et al. A multi-institutional study confirms the presence and expression of simian virus 40 in human malignant mesotheliomas. Cancer Res 1999;58:4505–9.
15. Carbone MC, Rizzo P, Grimley PM, et al. Simian virus-40 large-T antigen binds p53 in human mesotheliomas. Nat Med 1997;3:908–12.
16. De Luca A, Baldi A, Esposito V, et al. The retinoblastoma gene family pRb/p105, p107, pRb2/p130 and simian virus-40 large T-antigen in human mesotheliomas. Nat Med 1997;3:913–6.
17. Vivo C, Lecomte C, Levy F, et al. Cell cycle checkpoint status in human malignant mesothelioma cell lines: response to gamma radiation. Br J Cancer 2003;88:388–95.
18. Cistulli CA, Sorger T, Marsella JM, Vaslet CA, Kane AB. Spontaneous p53 mutation in murine mesothelial cells: increased sensitivity to DNA damage induced by asbestos and ionizing radiation. Toxicol Appl Pharmacol 1996;141:264–71.
19. Vaslet CA, Messier NJ, Kane AB. Accelerated progression of asbestos-induced mesotheliomas in heterozygous $p53^{+/-}$ mice. Toxicol Sci 2002;68:331–8.
20. Heineman EF, Bernstein L, Stark AD, Spirtas R. Mesothelioma, asbestos, and reported history of cancer in first-degree relatives. Cancer 1996;77:549–54.
21. Fung H, Kow YW, Van Houten B, et al. Asbestos increases mammalian AP-endonuclease gene expression, protein levels, and enzyme activity in mesothelial cells. Cancer Res 1998;58:189–94.
22. Broaddus VC, Yang L, Scavo LM, Ernst JD, Boylan AM. Asbestos induces apoptosis of human and rabbit pleural mesothelial cells via reactive oxygen species. J Clin Invest 1996;98:2050–9.
23. Schmitt CA, Fridman JS, Yang M, et al. A senescence program controlled by p53 and p16INK4a contributes to the outcome of cancer therapy. Cell 2002;109:335–46.
24. Johnstone RW, Ruefli AA, Lowe SW. Apoptosis: a link between cancer genetics and chemotherapy. Cell 2002; 108:153–64.
25. Shay JW, Roninson IB. Hallmarks of senescence in carcinogenesis and cancer therapy. Oncogene 2004;23: 2919–33.
26. Goodglick LA, Vaslet CA, Messier NJ, Kane AB. Growth factor responses and protooncogene expression of murine mesothelial cell lines derived from asbestos-induced mesotheliomas. Toxicol Pathol 1997;25:565–73.
27. Parris CN, Seidman MM. A signature element distinguishes sibling and independent mutations in a shuttle vector plasmid. Gene 1992;117:1–5.
28. Moalli PA, Macdonald JL, Goodglick LA, Kane AB. Acute injury and regeneration of the mesothelium in response to asbestos fibers. Am J Pathol 1987;128:426–45.
29. Dimri GP, Lee X, Basile G, et al. A biomarker that identifies senescent human cells in culture and in aging skin *in vivo*. Proc Natl Acad Sci U S A 1995;92:9363–7.
30. Murthy SS, Testa JR. Asbestos, chromosomal deletions, and tumor suppressor gene alterations in human malignant mesothelioma. J Cell Physiol 1999;180:150–7.
31. Xio S, Li D, Vijg J, Sugarbaker DJ, Corson JM, Fletcher JA. Codeletion of p15 and p16 in primary malignant mesothelioma. Oncogene 1995;11:511–5.
32. Pipas JM, Levine AJ. Role of T antigen interactions with p53 in tumorigenesis. Semin Cancer Biol 2001;11: 23–30.
33. Okayusu R, Takahashi S, Yamada S, Hei TK, Ullrich RL. Asbestos and DNA double strand breaks. Cancer Res 1999;59:298–300.
34. Sedelnikova OA, Rogakou EP, Panyutin IG, Bonner WM. Quantitative detection of ^{125}IdU-induced DNA double-strand breaks with γ-H2AX antibody. Radiat Res 2002;158:486–92.
35. Chen J, Stubbe J. Bleomycins: towards better therapeutics. Nat Rev Cancer 2005;5:102–12.
36. Cacciotti P, Barbone D, Porta C, et al. SV40-dependent AKT activity drives mesothelial cell transformation after asbestos exposure. Cancer Res 2005;65: 5256–62.
37. Robles SJ, Adami GR. Agents that cause DNA double strand breaks lead to p16INK4a enrichment and the premature senescence of normal fibroblasts. Oncogene 1998;16:1113–23.
38. Chang BD, Broude EV, Dokmanovic M, et al. A senescence-like phenotype distinguishes tumor cells that undergo terminal proliferation arrest after exposure to anticancer agents. Cancer Res 1999;59:3761–7.
39. Campisi J. Senescent cells, tumor suppression, and organismal aging: good citizens, bad neighbors. Cell 2005;120:513–22.
40. Yang CT, You L, Uematsu K, Yeh CC, McCormick F, Jablons DM. p14(ARF) modulates the cytolytic effect of ONYX-015 in mesothelioma cells. Cancer Res 2001; 61:5959–63.
41. Smythe WR, Hwang HC, Amin KM, et al. Use of recombinant adenovirus to transfer the herpes simplex virus thymidine kinase (HSVtk) gene to thoracic neoplasms: an effective *in vitro* drug sensitization system. Cancer Res 1994;54:2055–9.
42. Digweed M, Demuth I, Rothe S, et al. SV40 large T-antigen disturbs the formation of nuclear DNA-repair foci containing MRE11. Oncogene 2002;21:4873–8.
43. Ray FA, Peabody DS, Cooper JL, Cram LS, Kraemer PM. SV40 T antigen alone drives karyotype instability that precedes neoplastic transformation of human diploid fibroblasts. J Cell Biochem 1990;42:13–31.
44. Ke Y, Reddel RR, Gerwin BI, et al. Establishment of a human *in vitro* mesothelial cell model system for investigating mechanisms of asbestos-induced mesothelioma. Am J Pathol 1989;134:979–91.
45. Cicala C, Pompetti F, Carbone MC. SV40 induces mesotheliomas in hamsters. Am J Pathol 1993;142:1524–33.
46. Bocchetta M, Carbone M. SV40-mediated oncogenesis. In: Pass HI, Vogelzang NJ, Carbone M, editors. Malignant mesothelioma. New York: Springer; 2005. p. 34–59.
47. Altomare DA, You H, Ziao GH, et al. Human and mouse mesotheliomas exhibit elevated AKT/PKB activity, which can be targeted pharmacologically to inhibit tumor cell growth. Oncogene 2005;24:6080–9.
48. Ramos-Nino ME, Vianale G, Sabo-Attwood T, et al. Human mesothelioma cells exhibit tumor cell-specific differences in phosphatidylinositol 3-kinase/AKT activity that predict the efficacy of onconase. Mol Cancer Ther 2005;4:835–42.
49. te Poele RH, Okorokov AL, Jardine L, Cummings J, Joel SP. DNA damage is able to induce senescence in tumor cells *in vitro* and *in vivo*. Cancer Res 2002; 62:1876–83.
50. Foddis R, De Rienzo A, Broccoli D, et al. SV40 infection induces telomerase activity in human mesothelial cells. Oncogene 2002;21:1434–42.
51. Narita M, Nunez S, Heard E, et al. Rb-mediated heterochromatin formation and silencing of E2F target genes during cellular senescence. Cell 2003;113:703–16.
52. Campisi J. Suppressing cancer: the importance of being senescent. Science 2005;309:886–7.

SV40 Oncoproteins Enhance Asbestos-Induced DNA Double-Strand Breaks and Abrogate Senescence in Murine Mesothelial Cells

Jodie R. Pietruska and Agnes B. Kane

Cancer Res 2007;67:3637-3645.